X-621-74-254
PREPRINT

NASA TM X-70754

ARGON: A THERMOMETER OF THE UPPER ATMOSPHERE

S. CHANDRA
N. W. SPENCER

AUGUST 1974

GODDARD SPACE FLIGHT CENTER
GREENBELT, MARYLAND

ARGON: A THERMOMETER OF THE UPPER ATMOSPHERE

S. Chandra and N. W. Spencer
Laboratory for Planetary Atmospheres
Goddard Space Flight Center
Greenbelt, Maryland 20771

ABSTRACT

The exospheric temperatures are derived from Ar, N_2, O and He measurements obtained from the Aeros-1 NATE experiment. It is shown that the temperatures derived from Ar and N_2 are very close to each other and show very similar seasonal, latitudinal and the day to night variations both under quiet and the geomagnetically disturbed conditions. The temperatures derived from O and He do not usually follow this pattern because of their large variabilities in the lower thermosphere. The differences in the inferred temperatures from these gases are particularly noticeable when the neutral composition data between 220-250 km are used. In this altitude region Ar appears to have some advantage over N_2 for the purpose of deriving neutral temperature.

ARGON: A THERMOMETER OF THE UPPER ATMOSPHERES

S. Chandra and N. W. Spencer

Introduction

Our understanding of the thermal structure of the upper atmosphere has evolved largely from the vast amount of satellite drag data obtained over the past several years. Analysis of satellite drag data, of course, yields information about the total density at the perigee. The corresponding neutral temperature is derived by assuming diffusive equilibrium of all the neutral constituents above some reference level where the neutral composition and the temperature are specified and assumed invariant or nearly invariant under varying geophysical conditions (Jacchia 1965, 1971). The temperature derived from this technique is a very convenient index of the total density. Its usefulness as a representation of the neutral temperature is, however, questionable. When compared with the temperature measured from radar backscatter and airglow techniques, it gives a completely different picture of the diurnal, seasonal, and latitudinal variations of the thermospheric temperature (Salah and Evans 1973, Blamont, et al., 1974, Alcaydé, et al., 1974).

The basic difficulty in deriving exospheric temperature from satellite drag data lies in the fact that in the altitude region where most of the drag data are available, the total density corresponds mostly to the density of atomic oxygen. The assumption that atomic oxygen is invariant at a specified reference level (usually 120 km) in the lower thermosphere, is one of the weakest assumptions in deriving

temperature from the total density measurement. The observational data in the lower thermosphere, even though not very extensive, clearly indicate that atomic oxygen is highly variable under varying geophysical conditions (Donahue, et al., 1973; Alcaydé, et al., 1974; Reed and Chandra, 1974; also Johnson, 1973, for detailed references). This variability in [O] manifests itself as an error in the estimate of the thermospheric temperature.

The uncertainties in deriving thermospheric temperature from the neutral composition measurements can be minimized by choosing a neutral constituent which does not vary significantly in the lower thermosphere and whose variability produces minimum error under varying geophysical conditions.

The purpose of this paper is to show that of the four major neutral constituents (Ar, N_2, O and He) which are directly measured in the thermosphere, both Ar and N_2 satisfy these criteria better than O or He. The usefulness of N_2 in estimating thermospheric temperature has already been established from the OGO-6 Neutral Mass Spectrometer Measurement (Hedin et al., 1974). We shall show that Ar can be added to this list. In the altitude region below 250 km, where the variability at the lower boundary is likely to produce large error in the estimate of thermospheric temperature, Ar has some advantage over N_2. In this altitude region, the use of atomic oxygen in deriving temperature is marginal at best and probably incorrect. Helium, which has the largest seasonal and latitudinal variations gives maximum error in the estimate of the thermospheric temperature. It is, therefore, not

suitable for inferring neutral temperature. We shall support this argument by comparing the various geophysical features of the thermospheric temperature inferred from Ar, N_2, and O measured from the Aeros-1 NATE experiment.

Inferring Exospheric Temperatures from the Measurement of the Neutral Constituents

The procedure for estimating neutral temperature from the density measurement has been discussed by Jacchia (1965) and by Hedin, et al., (1974). The same approach can be adopted for estimating temperature from the individual neutral constituents. For an atmosphere in diffusive equilibrium, the distribution of the ith neutral constituent n_i, above a reference altitude z_o can be expressed by the following analytical expression (Walker, 1965):

$$n_i(z) = n_i(z_o) \left(\frac{To}{T}\right)^{1+\gamma_i+\frac{1}{\alpha H_\infty}} \exp\left(\frac{-\phi}{H_\infty}\right) \qquad (1)$$

where $$H_\infty = \frac{kT_\infty}{m_i g(z_o)}$$

$$T = T_\infty + (To - T_\infty) \exp(-\alpha\phi) \qquad (2)$$

$$\phi = \text{geopotential height} = \frac{(z-z_o)(R+z_o)}{(R+z)}$$

$g(z_o)$ = acceleration due to gravity at z_o

R = radius of the Earth

The other symbols in equations (1) and (2) denote the following: T_∞, T_o and α respectively denote exospheric temperature, temperature at

reference level (z_o) and the temperature gradient parameter as defined by Jacchia (1965); R, k, m; are respectively; the Earth's radius, the Boltzmann constant and the mass of the ith constituent. Finally, γ_i is the thermal diffusion coefficient which is assumed to equal to -0.38 for He and zero for all the other constituents.

It is evident from equations (1) and (2) that if $n_i(z_o)$, T_o and α are known, the temperature above a reference level can be uniquely determined from the density measurement at any given altitude. To illustrate the nature of the error resulting from the selected constituent quantitatively, we have shown in Figures 1a and 1b, the effect of changing neutral constituents at the lower boundary. We have assumed a model atmosphere with T_∞ = 1000°K, and the other parameters as follows: z_o = 120 km, T_o = 355°K, $[N_2]_{z_o} = 4 \times 10^{11}$ cm^{-3} and $[Ar]_{z_o} = 2 \times 10^9$ cm^{-3}. In Figure 1a are shown the ranges of variation in T_∞ inferred from the model values of N_2 at 400, 300, and 200 km. With the change in N_2 from 2×10^{11} cm^{-3} to 8×10^{11}cm^{-3}, the range of inferred temperature changes with the altitude. At 400 km, this range is from 1100°K to 950°K indicating an overall error of 10 per cent or less from the reference value of 1000°K. With the decrease in altitude, the range of variability increases and becomes very large at 200 km. The temperature inferred from other gases show the same characteristics, i.e., for all the gases the range of variability or error in the estimate of T_∞ increases with the decrease in altitude.

In Figure 1b, we have shown the variability in T_∞ inferred from Ar, N_2, and O, when their number densities at the lower boundary are changed

from their respective model values by an arbitrary factor. For illustration, we have chosen a reference altitude at 300 km, though similar inferences can be made from any altitude. We note in this figure that by varying the lower boundary by the same factor, T_∞ varies the least for Ar followed by N_2 and O. In fact, temperatures inferred from N_2 and A_r are very close to each other and differ significantly from O.

Thus, if the density of Ar, N_2, and O at 120 km varied by the same amount, the error in deducing temperature is least for Ar. Helium, of course, would lead to the largest error (not shown in Figure 1b) and cannot be used as an indicator of temperature in this altitude range.

From geophysical considerations, Ar is preferable over other gases. By solving a system of coupled equations involving equations of continuity and energy balance, Sinha and Chandra (1974) have shown that both He and O are subject to considerable variability in the lower thermosphere due to changes in eddy diffusion coefficient. Compared to these constituents N_2 is less and Ar the least variable. The changes in eddy diffusion coefficient, of course, has no direct effect on N_2 which is a major constituent in the lower thermosphere ($z<130$ km). Its effect is indirect through temperature which is affected by the change in eddy conduction.

Comparison of Exospheric Temperatures Inferred from O, N_2 and Ar and O

In the previous section we have discussed relative merits of Ar, N_2 and O for the purpose of deriving neutral temperatures. In the following, we shall make a detailed comparison of temperatures inferred from these three gases under varying geophysical conditions. The

neutral composition d ata are obtained from the Aeros-1 NATE experiment. The Aeros-1 was launched on December 16, 1972, in a polar orbit having fixed local times of about 1500/0300 hours. The satellite had a perigee of 220 km and an apogee of 865 km. The NATE experiment which was designed primarily to make in-situ measurements of temperature also functioned in an alternate mode as a neutral mass spectrometer to measure Ar, O, N_2 and He densities.

The basic principle of the experiment, its design and its mode of operation has been discussed by Spencer et al., (1974) and will not be repeated here. Unfortunately, because of the difficulty in the timing system of the spacecraft, proper synchronization of the data frame with the spin position was not achieved - a requirement essential for the analysis of the data in the temperature mode. The instrument, however, performed quite well as a mass spectrometer throughout the life period of the spacecraft and a good quality N_2, O and He data were obtained from perigee to an altitude range of 500 - 600 km. For Ar, the signal/noise ratio decreased rapidly above 350 km and useful data were obtained only up to that altitude.

Exospheric temperatures inferred from O, N_2 and Ar (T_∞ (O), $T_\infty(N_2)$, T_∞(Ar)), using equations (1) and (2), are shown in Figures 2a, 2b, and 2c. The temperatures are plotted against geodetic latitude with the altitude of the satellite shown on a running scale. Figures 2a and 2b respectively represent the winter and the summer conditions in the northern hemisphere. Figure 2c represents an equinox condition. In each of the three figures, the positions of the perigee is indicated by an

arrow. The local times shown in the captions correspond to the equator. The local times between $\pm$ 60° latitudes differ by two hours approximately. The boundary values used in deriving these temperatures are as follows:

z_o = 120 km, T_o = 355°K $[N_2]_{z_o} = 4 \times 10^{11}$ cm^{-3} $[O]_{z_o} = 1.0 \times 10^{11}$ cm^{-3}, $[Ar]_{z_o} = 2.0 \times 10^{9}$ cm^{-3}.

It is apparent from Figures 2a - 2c, that in the altitude region where temperatures inferred from the three gases can be compared simultaneously, both T_∞(Ar) and $T_\infty(N_2)$ are very close to each other but differ significantly from T_∞ (O). In agreement with the conclusions of the previous section, their differences are larger at low altitudes and decrease with an increase in altitude. By adjusting the value of $[O]_{z_o}$ it is possible to achieve better agreement between T_∞ (O) and $T_\infty(N_2)$ or T_∞ (Ar) in limited latitude region but not in the entire latitude region. To achieve an overall agreement, it is necessary to introduce a latitudinal/seasonal and temporal variations in $[O]_{z_o}$. Since the differences between T_∞ (N_2) and T_∞ (Ar) are small, under varying geophysical conditions, it is apparent that variabilities in $[N_2]_{z_o}$ and $[Ar]_{z_o}$ are not sufficient to cause an appreciable error in the estimate of T_∞.

A detailed comparison of T_∞ (N_2) and T_∞ (Ar) are made in Figure 3 for summer and winter conditions. The data presented in this figure corresponds to January 22 and May 26, 1973, which are magnetically quiet days and have approximately similar solar activity as indicated by the 10.7 cm flux (SF ≈ 100). The temperatures inferred from the two gases are plotted against geodetic latitude. The data points shown are from all the orbits which cover the entire longitude range. The solid lines are drawn to indicate the main trends and the longitudinal spread.

The most obvious feature of Figure 3 is the similarity between T_∞ (N_2) and T_∞ (Ar) with respect to their seasonal and latitudinal variations. Their overall differences are about 50°K, though for individual data

points, the differences may be larger. T_∞(Ar) is not shown with the same latitudinal coverage as $T_\infty(N_2)$ because Ar concentration is too low above 350 km. It is, nevertheless, reasonable to assume that the latitudinal and seasonal variations of T_∞ (Ar) are similar to that of $T_\infty(N_2)$. A large seasonal and latitudinal variations of about 40-50 per cent is apparent in $T_\infty(N_2)$ and we may infer similar variations from T_∞(Ar). Recently, vonZahn et al., (1973) have reported an order of magnitude enhancement in Ar from winter to summer at 270 km. Following the analogy of winter helium bulge, von Zahn et al., have characterized this observation as a summer argon bulge. Our observations on Ar are in general agreement with those of von Zahn et al. We believe, however, that the argon bulge is merely a reflection of the enhancement of exospheric temperature from winter to summer and is analogous to the summer N_2 bulge.

A comparison between T_∞(Ar) and $T_\infty(N_2)$ for the equinox condition is made in Figure 4. The data corresponds to March 15, 1973, with a local time of about 0300 hours. The general scheme for the presentation of the data is the same as in Figure 3. Except in the high latitude region where T_∞(Ar) is slightly higher than $T_\infty(N_2)$, the overall agreement between them is very good. The temperatures inferred from both the gases have the same latitudinal characteristics even in the finer details.

The variations of exospheric temperatures inferred from Ar and N_2 from quiet to disturbed conditions are shown in Figure 5, the data in this figure corresponding to January 7 and January 10, 1973, which are

respectively magnetically quiet and disturbed days. The daily sum of K_p for the two days are respectively 15 and 32 and the corresponding decimeter fluxes are 116 and 107. The temperatures in Figure 5 are plotted against invariant latitude with magnetic north pole in the center. The local times on the left and the right side from the center correspond approximately to 0300 and 1400 hours respectively. The local time within 20° from the north pole is, of course, changing over a wide range. The temperatures inferred from both Ar and N_2 have basically the same geophysical information though on the average, $T_\infty(Ar)$ shows a larger scatter and slightly higher temperature than $T_\infty(N_2)$. The inferred temperatures from both the gases are lowest in the polar region during a quiet condition. The same region during the magnetic storm becomes most activated with temperature rising from about 700°K to about 1000°K. The effect of the magnetic storm, however, is confined only to high latitudes, the mid and low latitude regions not being affected significantly. During severe disturbances, the temperature rise inferred both from Ar and N_2 are as much as 1000°K or even more, and although progressively decreasing, the effect extends to very low latitudes. These conclusions are in general agreement with those arrived at by Blamont and Luton (1972) from OGO-6 airglow temperature measurements.

From the measurement of O and He number densities at the spacecraft altitude, we may estimate their number densities at any altitude using appropriate values of either $T_\infty(N_2)$ or $T_\infty(Ar)$. In Figure 6, we have shown the inferred variations in O and He at 120 km for the quiet and disturbed conditions corresponding to Figure 5, using appropriate values

of $T_\infty(N_2)$. The basic features are the same if $T_\infty(Ar)$ instead of $T_\infty(N_2)$ is used. The choice of $T_\infty(N_2)$, of course, giving a much larger latitudinal coverage. During the quiet condition, He shows a pronounced bulge in the high latitude region characteristic of the winter helium bulge. Atomic oxygen shows a similar bulge, though less pronounced and slightly displaced towards the lower latitudes. During the period of magnetic disturbance, both O and He show a marked depression in the polar region, giving the appearance of a shift of their bulges to the lower latitudes.

Summary and Conclusion

In this paper, we have discussed the derivation of thermospheric temperature from the neutral density data. In particular, we have discussed the relation of the changes in the lower boundary and the resulting errors in the estimate of thermospheric temperature from Ar, N_2, O and He. We have shown that of the four neutral constituents measured from the Aeros-1 NATE experiment, Ar is less susceptible to this error with N_2, O and He in turn having increasing susceptability. Exospheric temperatures inferred from Ar and N_2 assuming invariant boundary conditions, however, do not differ significantly under varying geophysical conditions. General characteristics of the thermosphere with respect to the seasonal, latitudinal and magnetic storm related changes in the exospheric temperature, inferred from both Ar and N_2, are the same and consistent with the results obtained from radar backscatter, doppler airglow temperature, and OGO-6 model.

REFERENCES

Alcaydé, D., P. Bauer and J. Fontanari, Long term variations of thermospheric temperature and composition, J. Geophys. Res., 79, 629, 1974.

Blamont, J. E. and J. M. Luton, Geomagnetic effect on the neutral temperature of the F-region during the magnetic storm of September 1969, J. Geophys. Res., 77, 3534, 1972.

Blamont, J. E., J. M. Luton and J. S. Nisbet, Global temperature distributions from OGO-6 6300Å airglow measurements, Radio Science, 9, 247, 1974.

Donahue, T. M., B. Guenther and Ronald J. Thomas, Distribution of atomic oxygen in the upper atmosphere deduced from OGO-6 airglow observations, J. Geophys. Res., 78, 6662, 1973.

Hedin, A. E., H. G. Mayr, C. A. Reber, N. W. Spencer and G. R. Carignan, Empirical model of global thermospheric temperature and composition based on data from OGO-6 quadrupole mass spectrometer, J. Geophys. Res., 79, 215, 1974.

Jacchia, L. G., Static diffusion models of the upper atmosphere with empirical temperature profiles, Smithson. Contrib. Astrophys., 8, 215, 1965.

Jacchia, L. G., Revised static models of the thermosphere and exosphere with empirical temperature profiles, Spec. Rep. 332, Smithson. Astrophys. Obs., Cambridge, Mass., 1971.

Johnson, F., Horizontal variations in thermospheric composition, Rev. of Geophys., 11, 741, 1973.

Reed, E. I. and S. Chandra, The global characteristics of atmospheric emissions in the lower thermosphere and their aeronomic implications, J. Geophys. Res. (submitted for publication).

Salah, J. E. and J. V. Evans, Measurements of thermospheric temperature by incoherent scatter radar, Space Res., 13, 268, 1973.

Sinha, A. K. and S. Chandra, Seasonal and storm related changes in the thermosphere induced by eddy mixing, J. Atmos. Terr. Phys., 36, 1974.

Spencer, N. W., D. T. Pelz, H. B. Niemann, G. R. Carignan and J. R. Caldwell, The neutral atmosphere temperature experiment, J. Geophys. 1974.

Von Zahn, U., K. H. Fricke, and H. Trinks, Esro 4 gas analyzer results: First observation on the summer argon bulge, J. Geophys. Res., 78, 7560, 1973.

Walker, J.C.G., Analytic representation of upper atmosphere densities based on Jacchia static diffusion models, J. Atmos. Sci., 22, 462, 1965.

FIGURE CAPTIONS

1a Exospheric temperatures inferred from N_2 by varying the density at 120 km from 2 x 10^{11} to 8 x 10^{11} cm^{-3}.

1b Exospheric temperatures inferred from O, N_2, and Ar, by varying their number densities by the same amount with respect to some reference values.

2a Comparison of exospheric temperatures inferred from O, N_2 and Ar from a single AEROS pass on January 22, 1973. Local time at the equator ∿1430 hours.

2b Comparison of exospheric temperatures inferred from O, N_2, and Ar from single AEROS pass on May 26, 1973. Local time at the equator ∿1430 hours.

2c Comparison of exospheric temperatures inferred from O, N_2 and A_r from a single AEROS pass on March 15, 1973. Local time at the equator ∿0300 hours.

3 Latitudinal variations of exospheric temperature inferred from N_2 and Ar for summer and winter daytime conditions.

4 Latitudinal variations of exospheric temperatures inferred from N_2 and Ar for an equinox nighttime condition.

5 Comparison of $T_\infty(Ar)$ and $T_\infty(N_2)$ for magnetically quiet and disturbed conditions.

6 Atomic oxygen and helium number densities at 120 km during magnetically quiet and disturbed conditions.

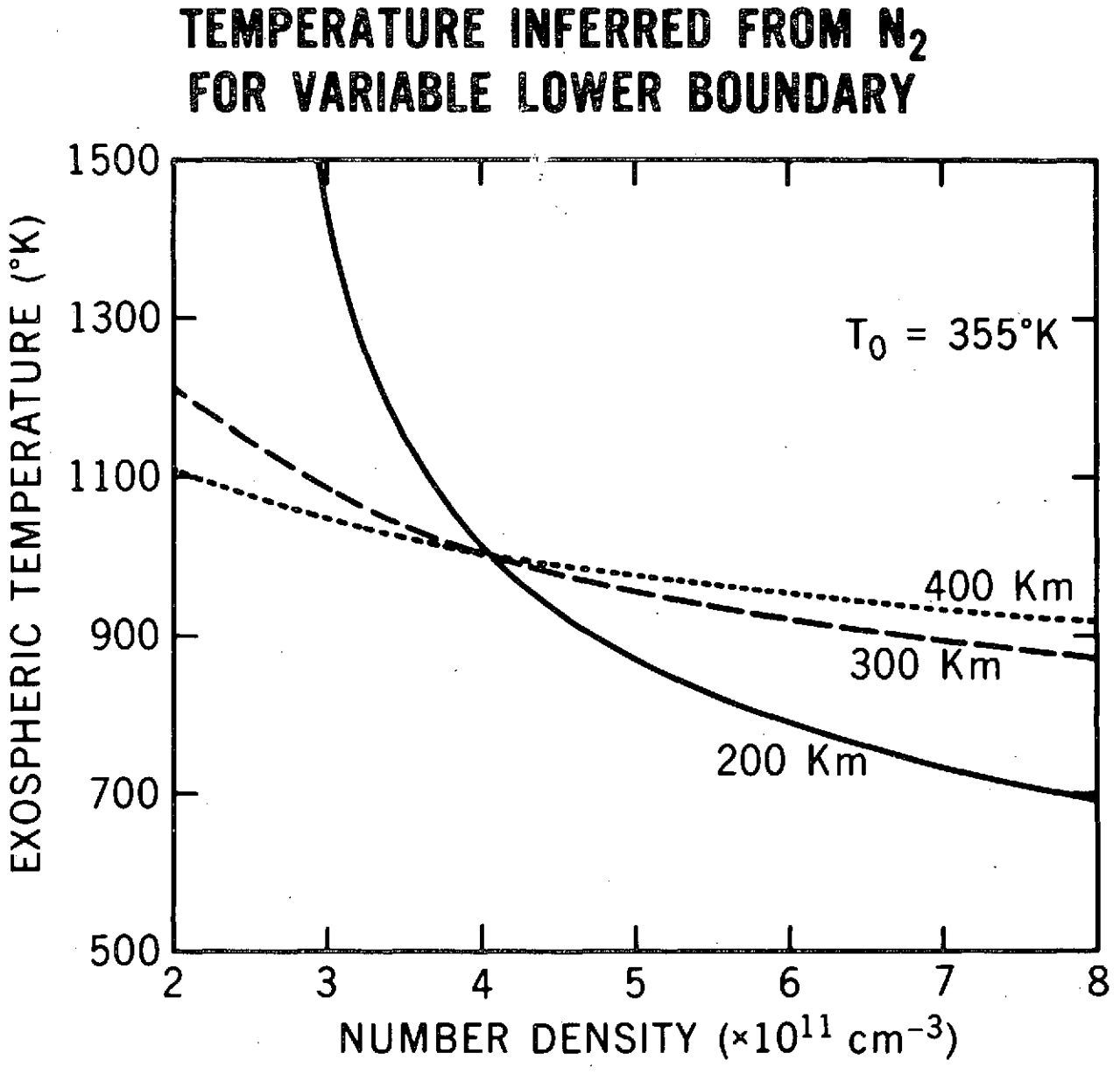
TEMPERATURE INFERRED FROM N_2
FOR VARIABLE LOWER BOUNDARY
EXOSPHERIC TEMPERATURE (°K)
1500
1300
1100
900
700
500
T_0 = 355°K
400 Km
300 Km
200 Km
2
3
4
5
6
7
8
NUMBER DENSITY ($\times 10^{11}$ cm^{-3})

Figure 1-a

TEMPERATURES INFERRED FROM O, N_2 AND Ar FOR VARIABLE LOWER BOUNDARY

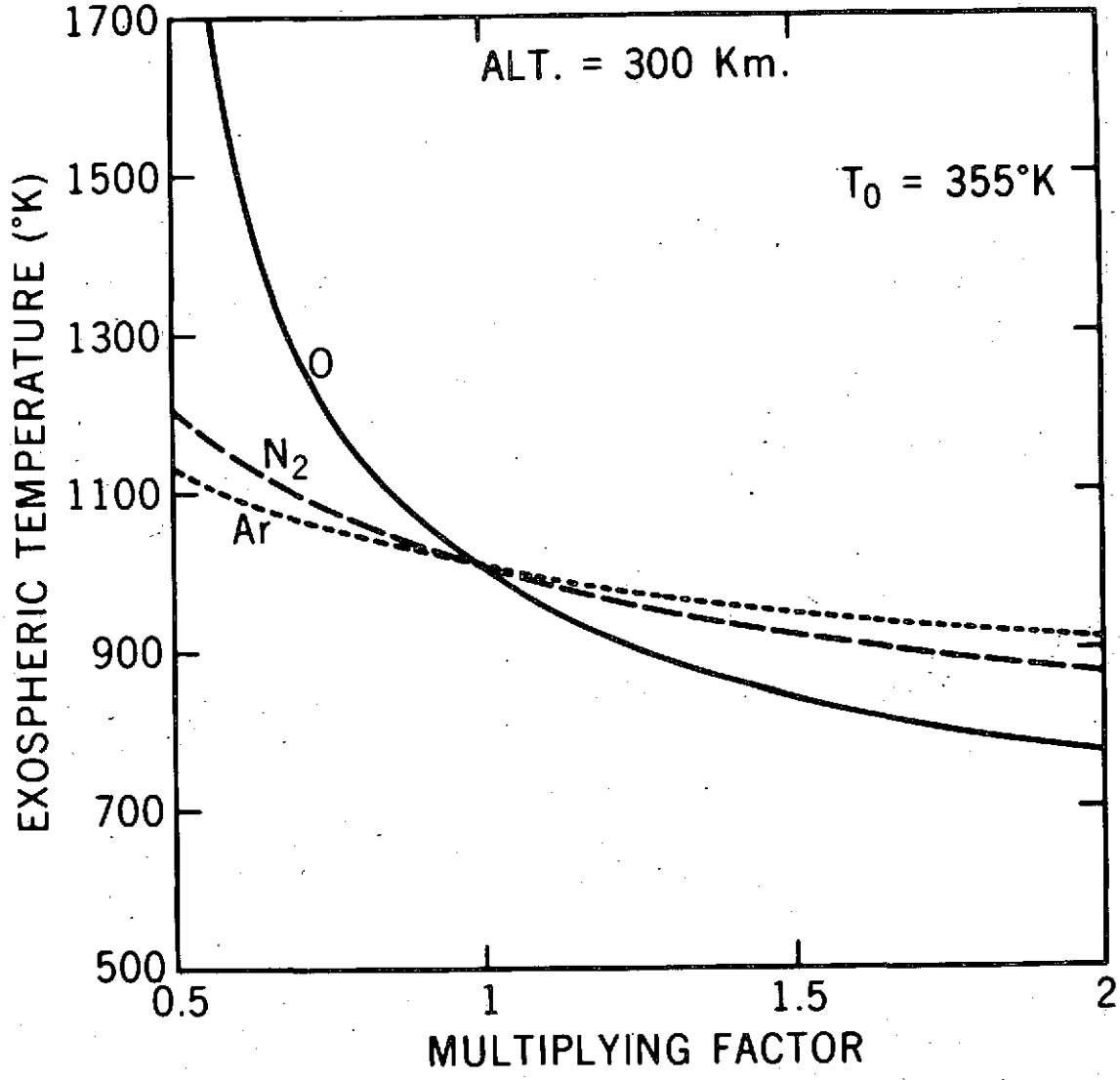

Figure 1-b

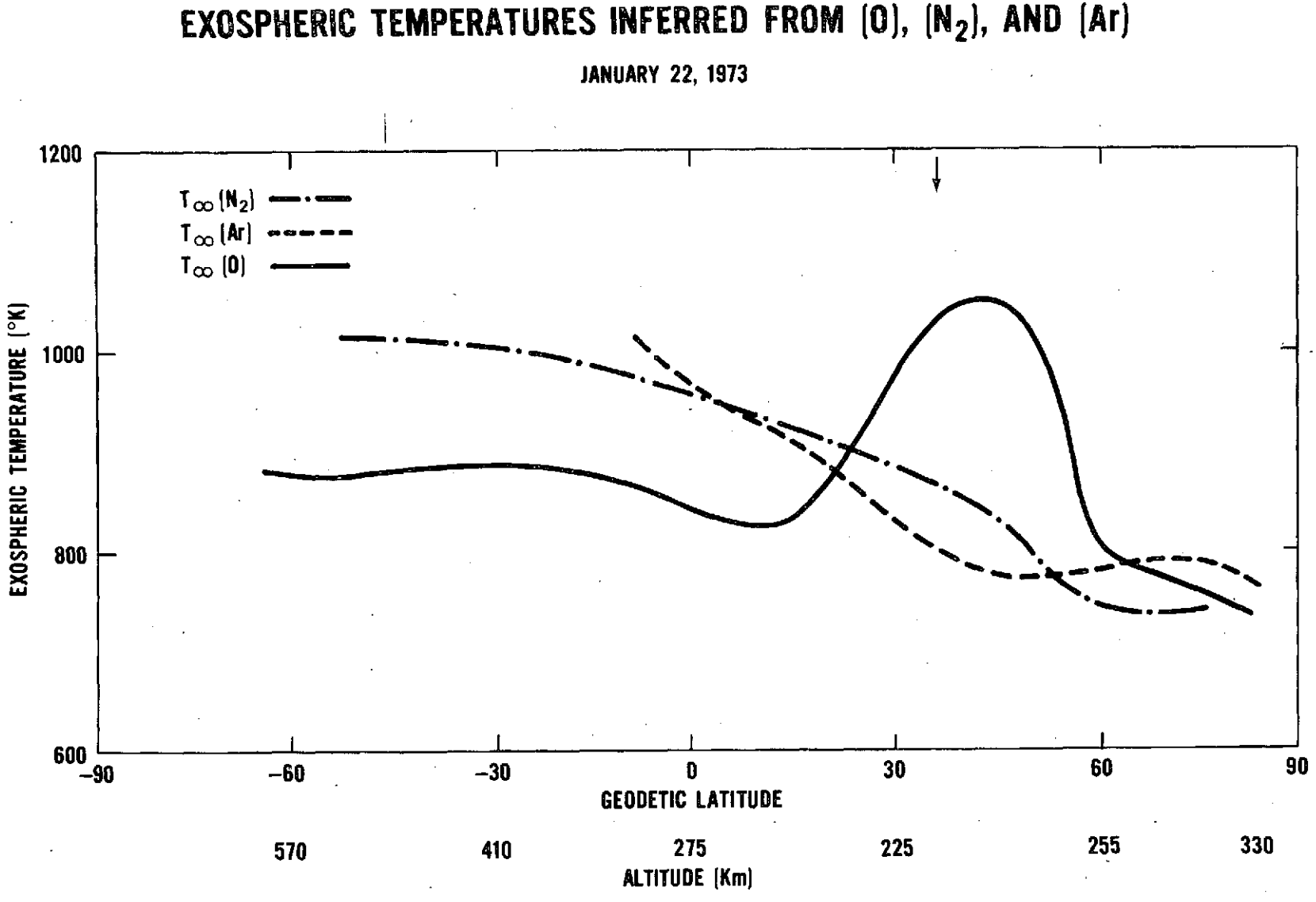
EXOSPHERIC TEMPERATURES INFERRED FROM (O), (N_2), AND (Ar)
JANUARY 22, 1973
T_∞ (N_2)
T_∞ (Ar)
T_∞ (O)
EXOSPHERIC TEMPERATURE (°K)
1200
1000
800
600
-90
-60
-30
0
30
60
90
GEODETIC LATITUDE
570
410
275
225
255
330
ALTITUDE (Km)

Figure 2-a

EXOSPHERIC TEMPERATURES INFERRED FROM (O), (N_2), AND (Ar)

MAY 26, 1973

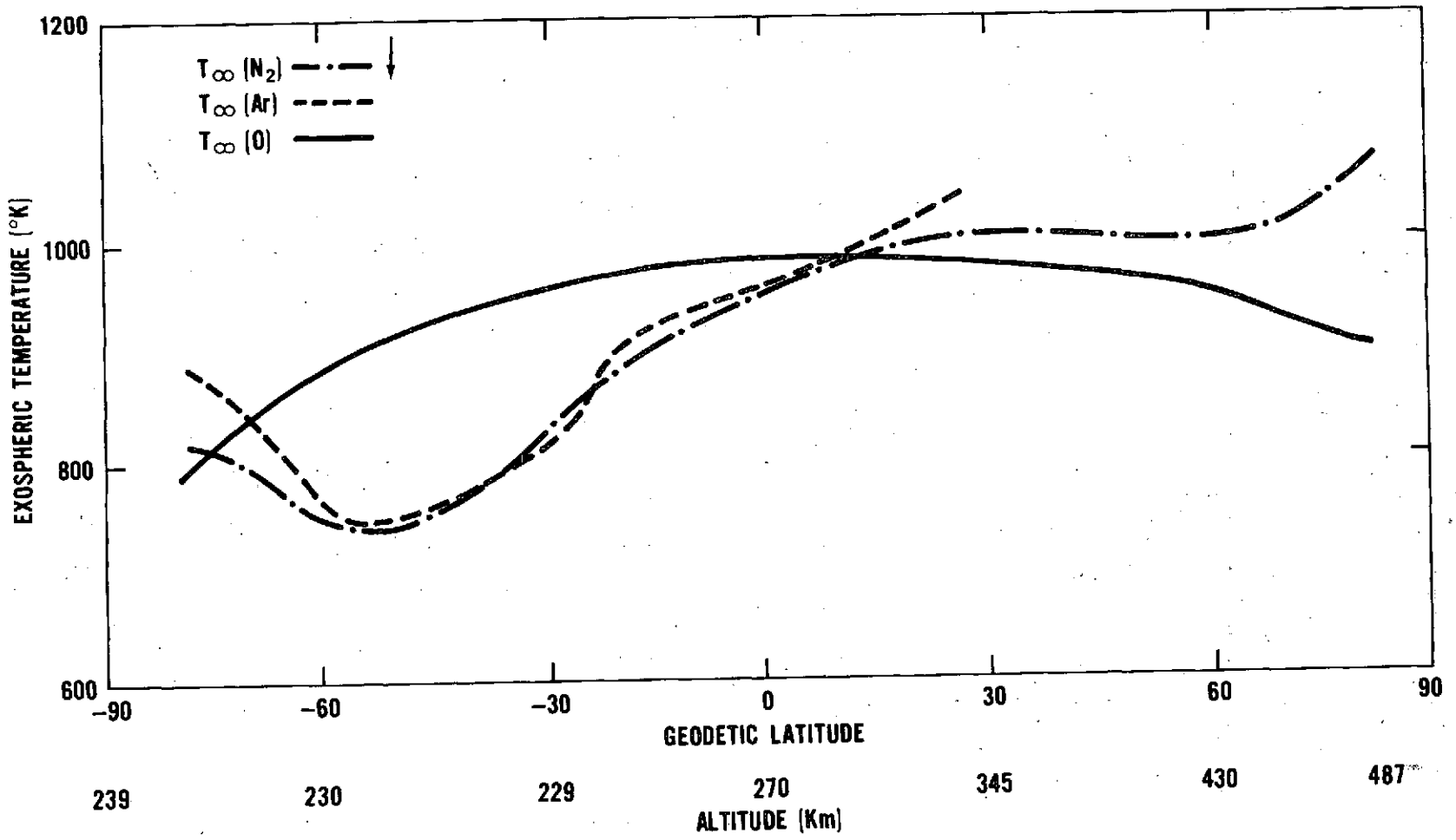

Figure 2-b

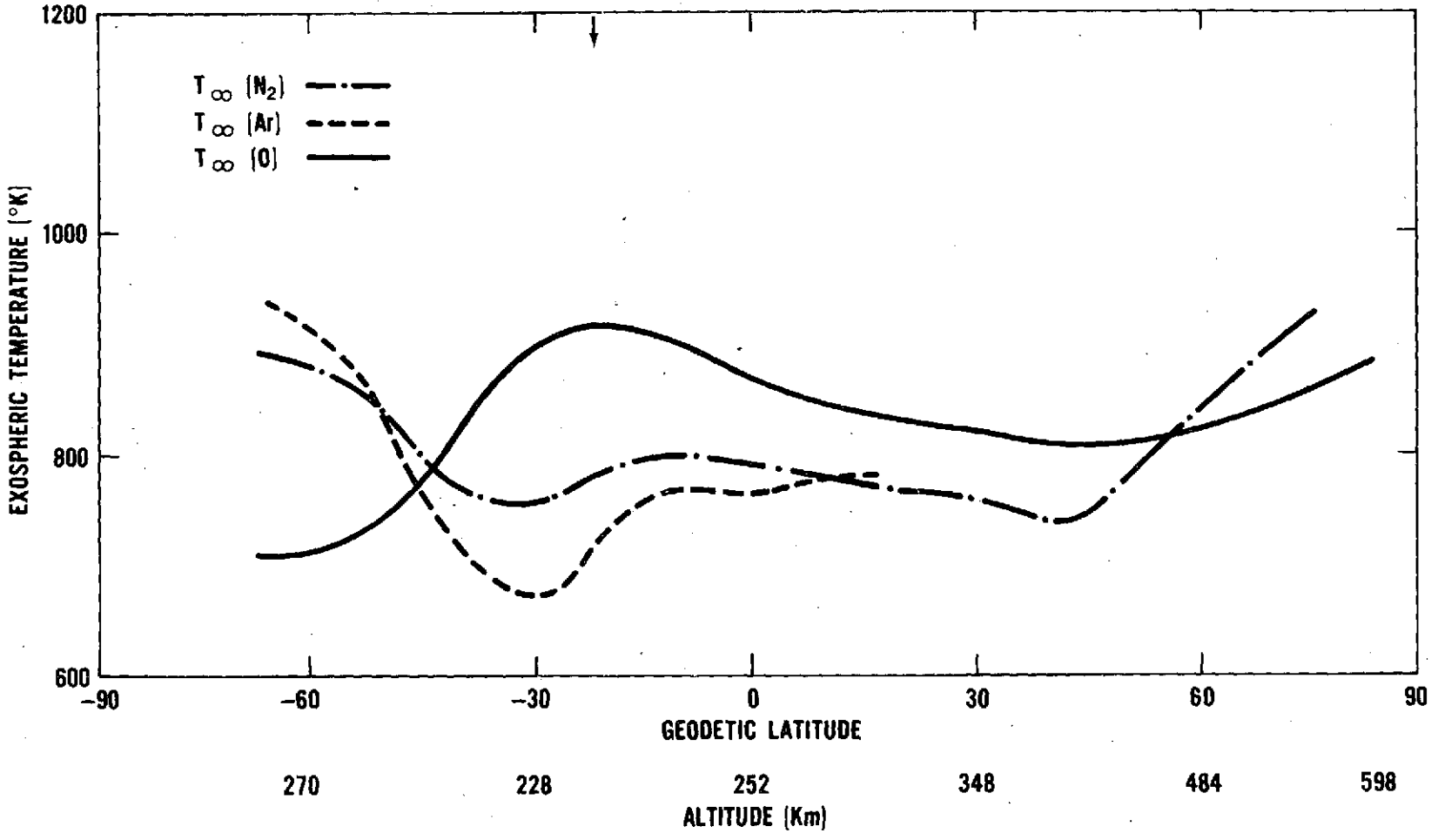
EXOSPHERIC TEMPERATURES INFERRED FROM (O), (N_2), AND (Ar)
MARCH 15, 1973
T_∞ (N_2)
T_∞ (Ar)
T_∞ (O)
EXOSPHERIC TEMPERATURE (°K)
1200
1000
800
600
-90
-60
-30
0
30
60
90
GEODETIC LATITUDE
270
228
252
348
484
598
ALTITUDE (Km)

Figure 2-c

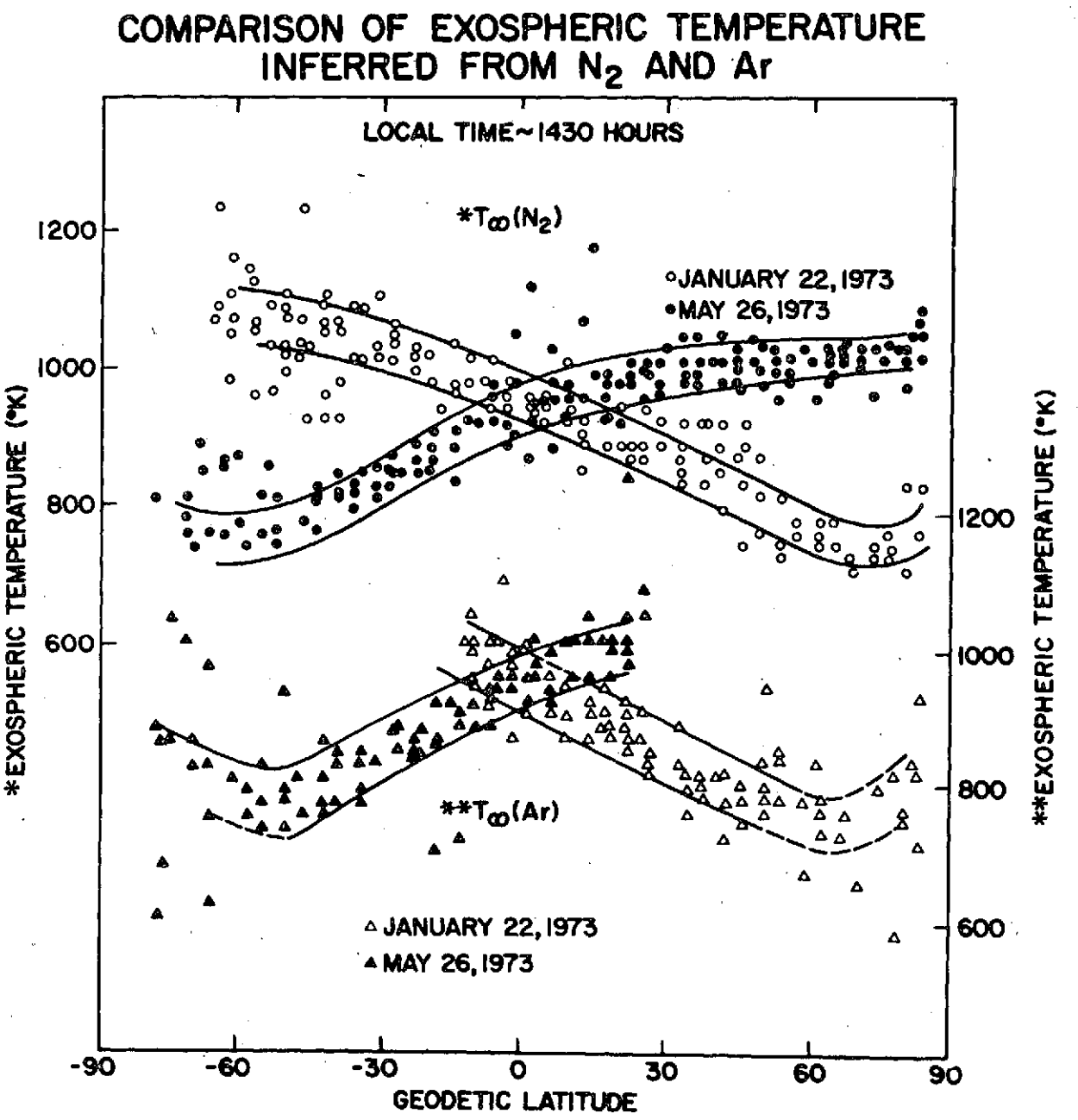
COMPARISON OF EXOSPHERIC TEMPERATURE INFERRED FROM N_2 AND Ar
LOCAL TIME~1430 HOURS
*$T_\infty(N_2)$
○JANUARY 22, 1973
●MAY 26, 1973
**T_∞(Ar)
△JANUARY 22, 1973
▲MAY 26, 1973
*EXOSPHERIC TEMPERATURE (°K)
**EXOSPHERIC TEMPERATURE (°K)
1200
1000
800
600
-90
-60
-30
0
30
60
90
GEODETIC LATITUDE

Figure 3

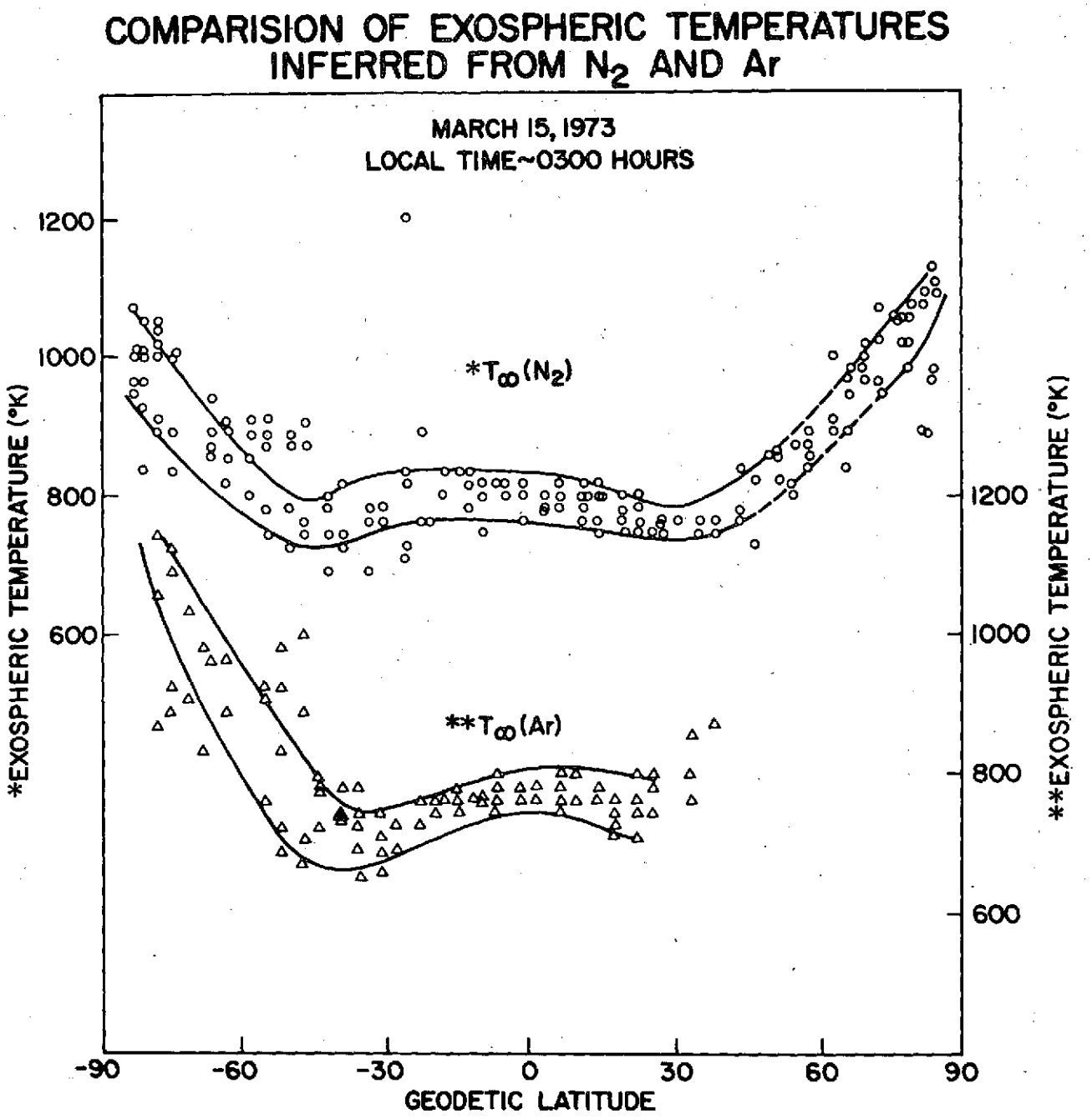
COMPARISION OF EXOSPHERIC TEMPERATURES
INFERRED FROM N_2 AND Ar
MARCH 15, 1973
LOCAL TIME~0300 HOURS
*$T_\infty(N_2)$
**T_∞(Ar)
*EXOSPHERIC TEMPERATURE (°K)
**EXOSPHERIC TEMPERATURE (°K)
1200
1000
800
600
-90
-60
-30
0
30
60
90
GEODETIC LATITUDE

Figure 4

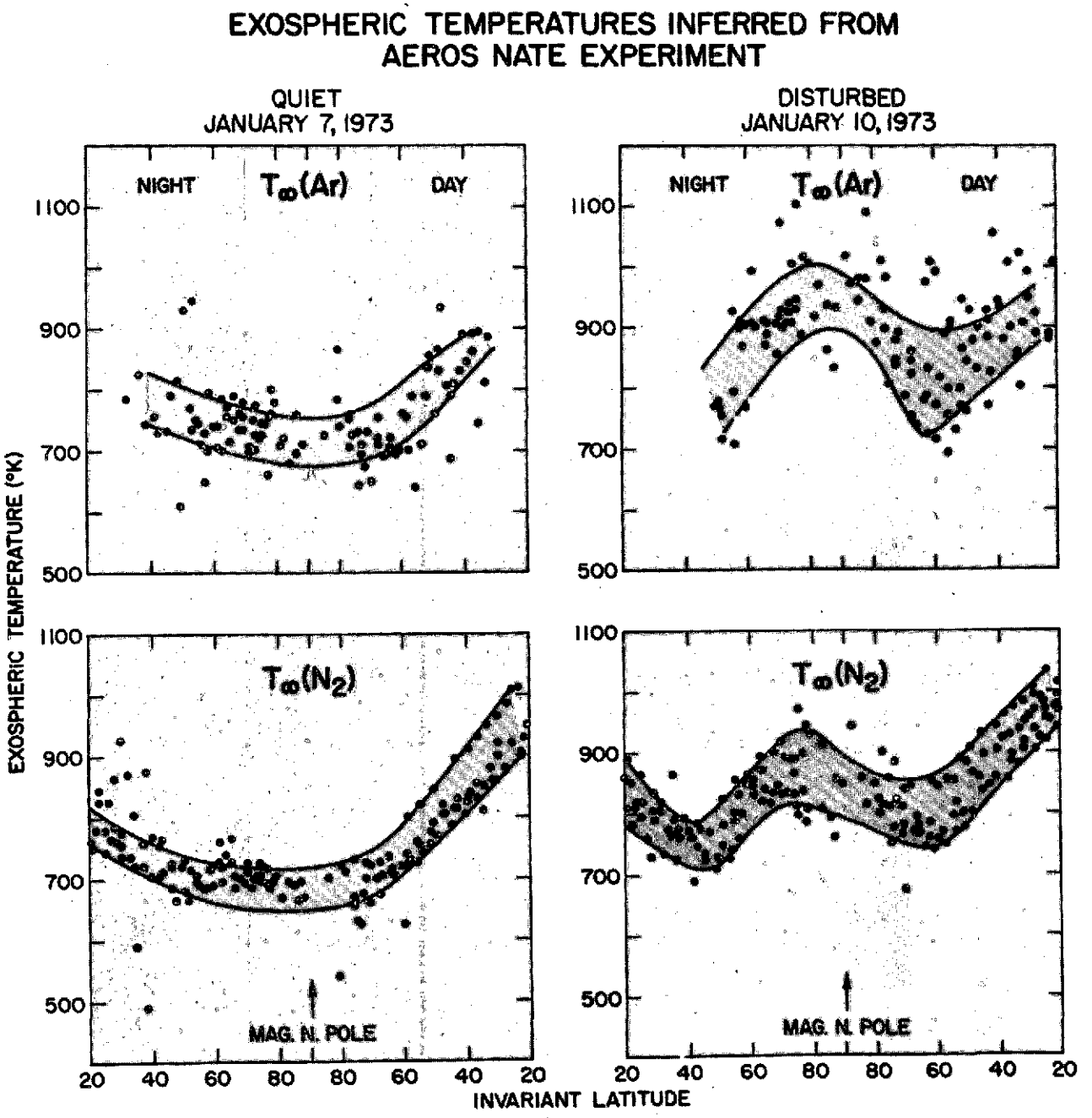
EXOSPHERIC TEMPERATURES INFERRED FROM AEROS NATE EXPERIMENT
QUIET
JANUARY 7, 1973
DISTURBED
JANUARY 10, 1973
NIGHT
$T_\infty(Ar)$
DAY
$T_\infty(N_2)$
MAG. N. POLE
EXOSPHERIC TEMPERATURE (°K)
INVARIANT LATITUDE
1100
900
700
500
20
40
60
80

Figure 5

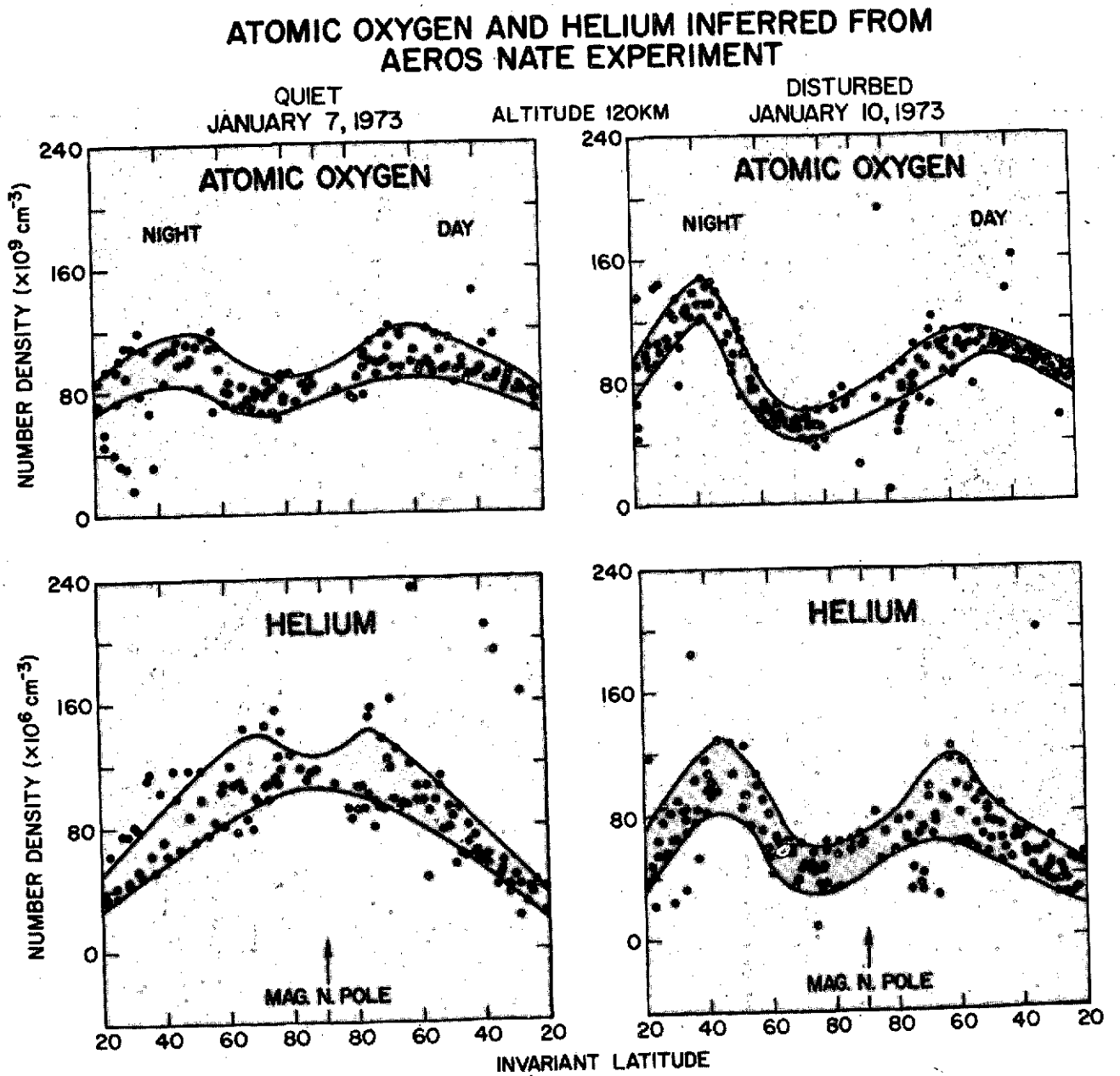
ATOMIC OXYGEN AND HELIUM INFERRED FROM AEROS NATE EXPERIMENT
QUIET
JANUARY 7, 1973
ALTITUDE 120KM
DISTURBED
JANUARY 10, 1973
ATOMIC OXYGEN
NIGHT
DAY
NUMBER DENSITY (×10⁹ cm⁻³)
240
160
80
0
HELIUM
NUMBER DENSITY (×10⁶ cm⁻³)
MAG. N. POLE
20 40 60 80 80 60 40 20
INVARIANT LATITUDE

Figure 6